Picosecond to femtosecond pulses from high power self mode-locked ytterbium rod-type fiber laser

Pierre Deslandes, Mathias Perrin, Julien Saby, Damien Sangla, François Salin, Eric Freysz

Picosecond to femtosecond pulses from high power self mode–locked ytterbium rod-type fiber laser

Pierre Deslandes, [1,2] Mathias Perrin, [2,3], Julien Saby,[1] Damien Sangla,[1] François Salin,[1] and Eric Freysz [2,3,*]

[1]*Eolite Systems, 11 avenue Canteranne, 33600 Pessac, France*
[2]*Université de Bordeaux, LOMA, UMR-5798, F 33400 Talence, France*
[3]*CNRS, LOMA, UMR 5798, F 33400 Talence, France*
[*]*e.freysz@loma.u-bordeaux1.fr*

Abstract: We have designed an ytterbium rod-type fiber laser oscillator with tunable pulse duration. This system that delivers more than 10 W of average power is self mode-locked. It yields femtosecond to picosecond laser pulses at a repetition rate of 74 MHz. The pulse duration is adjusted by changing the spectral width of a band pass filter that is inserted in the laser cavity. Using volume Bragg gratings of 0.9 nm and 0.07 nm spectrum bandwidth, this oscillator delivers nearly Fourier limited 2.8 ps and 18.5 ps pulses, respectively. With a 4 nm interference filter, one obtains picosecond pulses that have been externally dechirped down to 130 fs.

OCIS codes: (060.2320) Fiber optics amplifiers and oscillators: (140.3510) Lasers, fiber: (140.4050) Mode-locked lasers: (140.3615) Lasers, Ytterbium; (140.7090) Ultrafast lasers.

References and links

1. S. M. J. Kelly, "Characteristic sideband instability of periodically amplified average soliton," Electron. Lett. **28**(8), 806–807 (1992).
2. J. Limpert, N. Deguil-Robin, I. Manek-Hönninger, F. Salin, T. Schreiber, A. Liem, E. Röser, H. Zellmer, A. Tünnermann, A. Courjaud, C. Hönninger, and E. Mottay, "High-power picosecond fiber amplifier based on nonlinear spectral compression," Opt. Lett. **30**(7), 714–716 (2005).
3. A. Chong, W. H. Renninger, and F. W. Wise, "All-normal-dispersion femtosecond fiber laser with pulse energy above 20 nJ," Opt. Lett. **32**(16), 2408–2410 (2007).
4. C. Lecaplain, M. Baumgartl, T. Schreiber, and A. Hideur, "On the mode-locking mechanism of a dissipative-soliton fiber oscillator," Opt. Express **19**(27), 26742–26751 (2011).
5. W. H. Renninger, A. Chong, and F. W. Wise, "Amplifier similaritons in a dispersion-mapped fiber laser [Invited]," Opt. Express **19**(23), 22496–22501 (2011).
6. B. Ortaç, M. Baumgartl, J. Limpert, and A. Tünnermann, "Approaching microjoule-level pulse energy with mode-locked femtosecond fiber lasers," Opt. Lett. **34**(10), 1585–1587 (2009).
7. S. Lefrançois, K. Kieu, Y. Deng, J. D. Kafka, and F. W. Wise, "Scaling of dissipative soliton fiber lasers to megawatt peak powers by use of large-area photonic crystal fiber," Opt. Lett. **35**(10), 1569–1571 (2010).
8. M. Baumgartl, F. Jansen, F. Stutzki, C. Jauregui, B. Ortaç, J. Limpert, and A. Tünnermann, "High average and peak power femtosecond large-pitch photonic-crystal-fiber laser," Opt. Lett. **36**(2), 244–246 (2011).
9. N. B. Chichkov, C. Hapke, K. Hausmann, T. Theeg, D. Wandt, U. Morgner, J. Neumann, and D. Kracht, "0.5 μJ pulses from a giant-chirp ytterbium fiber oscillator," Opt. Express **19**(4), 3647–3650 (2011).
10. M. Baumgartl, C. Lecaplain, A. Hideur, J. Limpert, and A. Tünnermann, "66 W average power from a microjoule-class sub-100 fs fiber oscillator," Opt. Lett. **37**(10), 1640–1642 (2012).
11. D. Turchinovich, X. Liu, and J. Laegsgaard, "Monolithic all-PM femtosecond Yb-fiber laser stabilized with a narrow-band fiber Bragg grating and pulse-compressed in a hollow-core photonic crystal fiber," Opt. Express **16**(18), 14004–14014 (2008).
12. M. Baumgartl, J. Abreu-Afonso, A. Díez, M. Rothhardt, J. Limpert, and A. Tünnermann, "Environmentally-stable picosecond Yb fiber laser with low repetition rate," Appl. Phys. B **111**(1), 39–43 (2013).
13. J. M. Dziedzic, R. H. Stolen, and A. Ashkin, "Optical Kerr effect in long fibers," Appl. Opt. **20**(8), 1403–1406 (1981).
14. Ph. Grelu and N. Akhmediev, "Dissipative solitons for mode-locked lasers," Nat. Photonics **6**(2), 84–92 (2012).
15. H. A. Haus, J. G. Fujimoto, and E. P. Ippen, "Structures for additive pulse mode locking," J. Opt. Soc. Am. B **8**(10), 2068–2076 (1991).
16. G. Martel, C. Chédot, A. Hideur, and Ph. Grelu, "Numerical Maps for Fiber Lasers Mode Locked with Nonlinear Polarization Evolution: Comparison with Semi-Analytical Models," Fiber Integr. Opt. **27**(5), 320–340 (2008).

#185913 - $15.00 USD Received 25 Feb 2013; revised 17 Apr 2013; accepted 20 Apr 2013; published 25 Apr 2013

17. W. H. Renninger, A. Chong, and F. W. Wise, "Self-similar pulse evolution in an all-normal-dispersion laser," Phys. Rev. A **82**(2), 021805 (2010).
18. G. P. Agrawal, *Nonlinear Fiber Optics* (Academic Press, 2001). See Eq. (6).1.15–16).

1. Introduction

Pulsed fiber lasers are widely used for micromachining applications because of their compactness, excellent beam quality, maintenance free operation and high wall plug efficiency. To avoid thermal damage and to minimize the heat affected zone induced during laser material processing; ultrafast pulses with duration in the picoseconds (ps) and femtosecond (fs) range are required. In most of the cases, these pulses have to be efficiently doubled or tripled in frequency. To optimize laser processing end-users are therefore seeking for compact and powerful lasers that deliver pulses at high repetition rate nearly Fourier limited and with widely tunable pulse duration. However, it is well known that, usually, nonlinear processes limit the pulsed fiber laser oscillator to modest output peak power [1]. To overcome these limitations master-oscillator power-amplifier (MOPA) taking advantage of amplifying fibers have been used [2]. One can also use the nonlinear polarization evolution (NPE) to design high average power fs fiber oscillators in normal dispersion regime [3,4]. Both dissipative soliton as well as similariton mode locking have been reported [3,5]. These techniques make it possible to design powerful and compact fiber lasers [6–9]. Along this line, an ytterbium fiber oscillator delivering pulse with duration of ~2.1 ps with energy of ~0.9 µJ at 76.5 MHz high repetition rate has been reported very recently [10]. Due to the total cavity dispersion the pulse were positively chirped and needed to be dechirped. Using efficient grating compressor outside the cavity, the pulse were dechirped to 91 fs. It is important to stress that most of the efforts using this technique have been devoted towards the development of fs oscillators. Then one may wonder if NPE can also be used to design compact and more powerful fiber laser delivering pulses with duration in the range of ~2 to ~20 ps [11,12]. In this contribution, we will present the design and the performances of a high power ytterbium rod-type fiber oscillator that delivers pulses that duration are almost limited by their spectral bandwith with adjustable duration ranging from 18.5 ps to 130 fs. This system is shown to deliver more-than 10 W of average power at 74 MHz. The pulse peak power ranges from 9 kW to 1.1 MW. Numerical simulations well accounts for the behavior of this oscillator. They offer possibilities to further scaled-up the performances of such fiber lasers.

2. Experimental set-up

Figure 1 presents the design of our ring cavity. It is constructed around a 0.75 m long LMA double clad ytterbium rod type fiber. Two slightly birefringent fibers are used. The first one generates femtoseconds and ~2 ps pulses. It has a core diameter of 50 µm that results in a mode-field diameter of ~50 µm at 1030 nm, and a pump clad diameter of 170 µm. A microscope image of its structure is shown in the inset of Fig. 1. The nonlinear coefficient of this fiber is estimated to be $g = 2\ 10^{-4}\ W^{-1}\ m^{-1}$. The second one, used to generate the ~20 ps pulses, is very similar but it has a core diameter of 35 µm that results in a mode-field diameter of ~24 µm at 1030 nm, and a pump clad diameter of 90 µm. Its nonlinear coefficient is estimated to be $g = 3.9\ 10^{-4}\ W^{-1}\ m^{-1}$. Nonlinear effects are expected to be enhanced in this fiber. The absorption coefficient of these LMA fibers at 976 nm is ~25 $dB.m^{-1}$. These fibers have been cleaved and polished with an angle of ~5°, and are pumped through a dichroïc mirror using a fiber coupled laser diode emitting up to 100 W at 976 nm. The travelling wave oscillation is ensured by an optical isolator (OI). The isolator's polarizing beam splitter is used as an output coupler. To ensure self mode locking and dissipative soliton formation, one quarter-wave plate, two half-wave plates and a spectral filter have been introduced in the cavity. For the generation of picosecond pulses, we have used two different high reflecting volume Bragg gratings (VBG), both centered at 1030 nm, and with 0.9 nm and 0.07 nm spectral full width at half maximum (FWHM). There are used slightly out of normal incidence and their reflection coefficient is higher than 99%. For femtosecond pulse generation, we have

#185913 - $15.00 USD Received 25 Feb 2013; revised 17 Apr 2013; accepted 20 Apr 2013; published 25 Apr 2013

used an interference filter centered at 1040 nm. It has a transmission >90% and 4 nm spectral FWHM. To ensure self-starting of our oscillator, we take advantage of the NPE that combined with the wave-plates and the OI acts as a nonlinear and partially transmitting mirror [13]. Adjusting the polarization state by turning the wave-plates, one can control both the laser output power and the mode-locking.

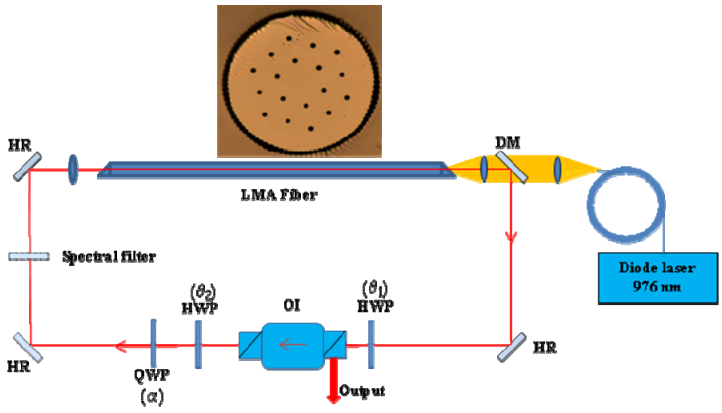

Fig. 1. Schematic representation of the experimental cavity set-up. DM, dichroïc mirror; HR high reflection mirror; OI optical isolator; QWP (HWP) quarter wave plate (Half wave plate). q_1,q_2 and a are the angleq of the wave plates. Inset microscope image of the structure of LMA fiber made by NKT photonics.

Whatever the spectral filter we used, we noticed the same laser behavior upon increasing the pump power. The typical behavior of our fs oscillator has previously been discussed [14]. Above a pump laser threshold, and for any angle of the wave-plates, the system works in CW regime and the laser intensity strongly fluctuates in time. At higher pump power, above the mode-locking threshold, and for a large range of parameters (pump power, wave-plate angles, bandwidth of spectral filter), the oscillator delivers a stable train of single or multiple pulses. The setting of the wave-plates for single pulse operation depends on the VBG or the spectral filter. However, with all the filters we used, we could observe self-starting mode-locking for pump power above 25 W. This relatively high threshold is due, firstly, to the short length of the used amplifying fiber, and to the weakness of its nonlinearity. However, once the filter is installed in the cavity and the wave plates are properly set, we could observe a single pulse at 74 MHz for pump powers up to 40 W. The mode locking regime remains stable over several hours; it is self-starting and very reproducible when the laser is turned off and on again. For pump power larger than 40 W, it delivers multiple pulses.

3. Experimental results

Generation of femtosecond pulses

The typical pulses sequence and beam profile yielded by our laser when we used the interference filter is shown in Fig. 2. In this figure, the two insets display the radio frequency spectrum recorded by a spectrum analyzer and the laser beam profile. The beam profile is gaussian with an M^2~1.1. The second inset shows a noise structure extending from −125 to + 125 kHz around the oscillator repetition rate revealing the very low noise amplitude of our oscillators. The corresponding energy fluctuation is estimated to be less than 0.9%. To check that the pulse train has no additional fine temporal structure, we have used a fast photo-diode and a 20 GHz sampling oscilloscope. This measurement did not reveal any pre- or post-pulse.

#185913 - $15.00 USD Received 25 Feb 2013; revised 17 Apr 2013; accepted 20 Apr 2013; published 25 Apr 2013

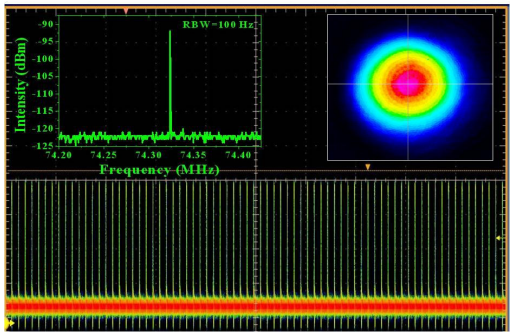

Fig. 2. Pulse train recorded on 20 GHz sampling oscilloscope (resolution 1 ns). Inset RF spectrum on a span of 250 kHz, resolution bandwidth (RBW) 100 Hz and laser beam profile (M^2~1.1).

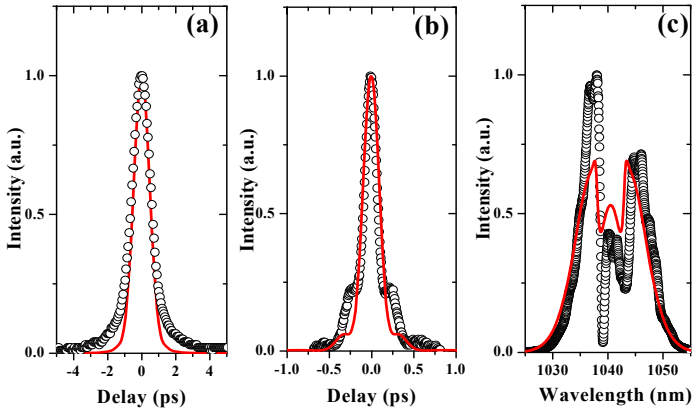

Fig. 3. Intensity autocorrelation traces of the chirped output pulse **(a)** and externally dechirped pulse **(b)** generated using a 4 nm spectral filter. **(c):** corresponding optical spectrum. Symbols show experimental data, solid lines show numerical results computed using the following parameters $\alpha = 220°$, $\theta_1 = 191°$ $\theta_2 = 174°$, $g_o = 8.5$ m^{-1}, $P_{Sat} = 1.1$ W. The dechirped numerical autocorrelation trace **(b)** has been computed assuming all the spectral components of the numerical spectrum **(c)** are in phase.

We have also measured the average power, the pulse spectrum and the pulse duration at the laser output. We could extract more than 10 W of average power. At 74 MHz repetition rate, this corresponds to energy per pulse of ~150 nJ. The pulse duration was measured using an intensity autocorrelator. Figures 3(a)-3(c) show the autocorrelation trace and the output pulse spectrum. The spectrum is structured and has a half-width of ~12 nm [Fig. 3(c)]. The output pulse duration is ~1 ps. The time-bandwidth product (i.e. Dn*Dt) of theses pulses is ~3.4 indicating the pulse duration is clearly not limited by its spectrum (Dn*Dt~0.44 for Gaussian pulses). However, we can easily compress the output pulse temporally, using a set of two negatively chirped highly reflective mirrors. They have a reflectivity R>99%, and a group velocity dispersion (GVD) of F_2~-10000 fs^2 at 1030 nm. As shown in Fig. 3(b), after three reflections, more than 98% of the initial pulse energy was transmitted and the pulse duration was 130 ± 10 fs close and time-bandwidth product is ~0.44, the expected value for Fourier transform Gaussian pulses. The autocorrelation trace of the compressed pulse was clean but exhibits some pedestals. They are very likely related to structure of the pulse spectrum. Indeed as shown in Fig. 3(b) the autocorrelation trace computed from the numerical model, considering that the spectral components of the pulse are in phase has similar pedestals and resembles the experimental one. The energy carried by the experimental pulse pedestals

#185913 - $15.00 USD Received 25 Feb 2013; revised 17 Apr 2013; accepted 20 Apr 2013; published 25 Apr 2013

was estimated to be ~20%. By increasing the pump power up to 33 W, we were able to keep the ~130 fs pulse duration and achieved an averaged output power of 11 W. The peak power of these dechirped pulses is ~1.1 MW.

To characterize more precisely our laser, we have also measured, thanks to the very small transmission through the calibrated HR mirrors, the average power, the spectrum and the pulse duration, at different points inside the cavity. It turns out that, up to 6 W are lost by the spectral filter. This corresponds to ~55% of the power at the OI output. Using mirrors with small and known transmission, we estimated the intra-cavity power to be 2.3 W at the input and 22 W at the exit of the amplifying fiber. This indicates that single pass saturated gain is ~10. A large part of the gain is used to compensate for the loss introduced by the interference filter. In agreement with previous work, we could easily lower these intracavity losses by increasing the spectral width of the interference filter [9]. The pulse spectrum measured at the exit and the input of the fiber as well as the spectrum rejected and transmitted by this filter is shown in Fig. 4. These results indicate that the pulse spectrum strongly evolves during its propagation within the laser cavity. However we noticed that the measured pulse duration is ~1 ps and it remains almost unchanged within the cavity. This stresses that our laser is indeed working in the normal-dispersion regime [3]. With 10 W of output power, knowing the pulse duration, the laser repetition rate, the nonlinear coefficient of the fiber and the average power at input and exit of the fiber, we evaluated the nonlinear phase shift to be ~4.3 p after a single pass in the fiber. This value is consistent with the modulated spectrum we measured at the exit of the fiber [Fig. 3(c)].

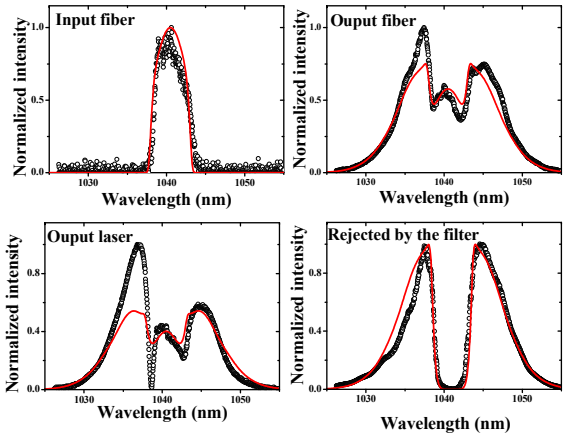

Fig. 4. Symbols: Experimental optical spectrum recorded at different points within the laser cavity using the 4 nm FWHM spectral filter, centered at 1040 nm. Solid lines: spectrum computed using the parameters of Fig. 3.

Generation of picosecond pulses

As we mentioned previously, for the generation of picosecond pulses, we have used high reflecting VBG centered at ~1030 nm with 0.9 nm and 0.07 nm FWHM. The VBG with Dl = 0.9 nm (resp. 0.07 nm) was used in combination with the fiber with a core diameter of 50 µm (resp. 35 µm). The single pulses mode-locking was observed for similar pump power but with different angles of l/2 and l/4 wave-plates. The typical pulses sequence, power stability and beam profile yielded by our laser using the VBG are almost similar to the data shown in Fig. 2. The observation of a stable single pulse generation indicates that, NPE is large enough to ensure mode-locking. With the two VBG and for single-pulse mode-locking, the maximum output power is 12,5 W for 35 W of pump power. The spectrum and the intensity autocorrelation traces, we measured are presented in Fig. 5. The spectrum recorded using the 0.9 nm VBG presents the characteristic modulations induced by self-phase and cross-phase

#185913 - $15.00 USD Received 25 Feb 2013; revised 17 Apr 2013; accepted 20 Apr 2013; published 25 Apr 2013

modulations. Using the 0.07 nm VBG, the output pulse spectrum was smooth but its structure cannot be finely measured due to the resolution of our spectrometer (Dl~0.02 nm). The duration of the pulses produced using the VBG with Dl = 0.9 nm (resp. 0.07 nm) is equal to t = 2.8 ± 0.1 ps (resp 18.5 ± 0.5 ps). It is important to stress that, within our experimental uncertainties, the autocorrelation trace of these generated pulses does not exhibit noticeable pedestals [Fig. 5(b)-5(d)]. The time-bandwidth product of the 2.8 ps and 18.5 ps pulses are equal to 0.65 ± 0.02 and 0.45 ± 0.01 respectively. This indicates that as expected, as the duration of the generated pulses increases and the peak power decreases, the chirp introduced by the linear and nonlinear effect within the fiber have a lesser impact on the time-bandwidth product. For the maximum output power, the peak power generated by our fiber laser is ~60 kW and ~9 kW, for the 2.8 ps and 18.5 ps pulse respectively. Above 35 Watts of pump power, we observe multi-pulses or unstable regimes. Here again, with 12.5 W of output power, we could evaluate the nonlinear phase shift after a single pass in the fiber. We found it is ~1.5 p and p using 0.9 nm and 0.07 nm spectral filters respectively. They are consistent with the modulated spectrum reported in Fig. 5. These phase shifts shed light on the important role of nonlinear phase modulation that takes place in our laser. In this picosecond regime, two points have to be underlined.

a. The losses introduced by the VBG are considerably reduced compared to the ones introduced by the interference filter.

b. Keeping the pump power below 35 W, we tried but did not succeed to mode-lock our laser using fiber with a 50 µm core diameter and the 0.07 nm spectral filter. Thus considering that the pulse duration is mainly fixed by the VBG and the peak power are similar in the our two fibers, our results indicates the nonlinear phase shift of ~p/2 induced into the 50 µm core diameter fiber is not sufficient to ensure a reliable mode locking.

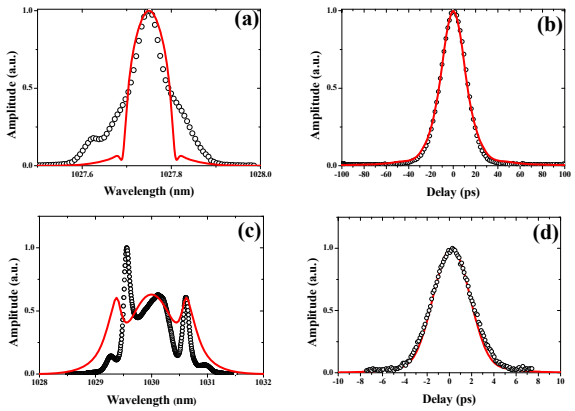

Fig. 5. Symbols:Experimental optical spectrum **(a,c)** and intensity autocorrelation traces **(b,d)** recorded using the 0.07 nm **(a,b)** and 0.9 nm **(c,d)** VBG mirrors. Solid lines: computed results. For Fig **(a, b)** we used the following parameters: $\alpha = 120°$, $\theta_1 = 105°$ $\theta_2 = 30°$, $g_o = 9\ m^{-1}$, $P_{SAT} = 2.3$ W. For Fig (**c,d**): $\alpha = 216°$, $\theta_1 = 191°$ $\theta_2 = 171°$, $g_o = 8.5\ m^{-1}$, $P_{SAT} = 1.1$ W

#185913 - $15.00 USD Received 25 Feb 2013; revised 17 Apr 2013; accepted 20 Apr 2013; published 25 Apr 2013

4. Numerical simulations and discussion

Table 1. recapitulative table that gathers the main experimental and simulation results. exp.: experimental, num.: numeric, unchirped: obtain after external dechirping.

Filters bandwidth at FWHM (nm)	γ (W^{-1} m^{-1})	Peak power (kW)	Average power (W)	Pulse width at FWHM (ps)	Pulse width at FWHM (nm)
4	***2 x 10^{-4}***	***137 (exp) 90 (num.) 1100 (unchirped)***	***11 (exp.) 7.2 (num.) 10.5 (unchirped)***	***1 ± 0.1 (exp.) 0.9 (num.) 0.12 (unchirped)***	***12 ± 0.2 (exp.) 13.8 (num.)***
0.9	***2 x 10^{-4}***	***60 (exp.) 56 (num)***	***12.5 (exp.) 11.7 (num.)***	***2.8 ± 0.2 (exp.) 2.85 (num.)***	***1.21 ± 0.02 (exp.) 1.42 (num.)***
0.07	***3.9 x 10^{-4}***	***9 (exp.) 8.6 (num.)***	***12.5 (exp.) 11.9 (num.)***	***18.5 ± 0.2 (exp.) 18 (num.)***	***0.09 ± 0.01 (exp.) 0.092 (num.)***

To get a deeper understanding, an original numerical vectorial model has been developed. Many models of fiber laser mode locking with NPE exist. Those based on a master equation [15], are valid when the effect per round trip is small enough, which is not the case here. Some others model the NPE by a saturable absorber with ad hoc saturation and absorption coefficients [3]. Then, a scalar Non-Linear Schrödinger Equation (NLSE) is used, and polarization evolution is overlooked. At last, some models treat sequentially the vectorial propagation in fiber and the polarization change due to all the other optical elements in the cavity (OI, wave plates) [16,17], as well as the spectral filtering. We have used such a vectorial NLSE to describe the pulse evolution in the gain fiber, which is weakly birefringent. For the two rod fibers that were used, the birefringence was indeed measured experimentally to be $\Delta n = 10^{-5}$. The complex field envelope evolves under the influence of self-phase modulation, cross-phase modulation, and coherent coupling between the two modes of polarization in the fiber [18]. The nonlinear coefficient γ has been computed from the mode field diameter (see Table 1), and the gain, g, is defined as $g = g_o/(1 + P/P_{sat})$, where g_o is the small signal gain, P is the total power, and P_{sat} is the saturation power. Both g_o and P_{sat} have been adjusted to fit quantitatively with experimental results. We obtain the same qualitative behavior over a wide range of values for g_o and P_{sat}.The group velocity dispersion is $\beta_2 = 0.025$ ps^2 m^{-1}.

We have computed the pulse evolution in the fiber using a standard third order split step method. The Jones formalism has been used to model how the pulse evolves when passing through the wave plates and the optical isolator. Note that all the waveplate angles are measured by respect to the rejection axis of the OI. They are denoted: α for the quarter wave plate, θ_1 for the half wave plate situated before OI, and θ_2 for the one situated afterwards. The spectral filtering is modeled by a Gaussian transmission function that acts on the spectral amplitude, without introducing chirp. At the difference of [16], we do not have any dispersive element except the fiber, and we consider a filtering much narrower than the gain bandwidth (~40 nm). At the difference of [17], we operate in a regime with a much smaller total dispersion, and the fiber has a weak birefringence. During the computations, we tuned the angle of the wave-plates and we varied the pump power, checking carefully the convergence towards a stable steady state, independent of the initial condition. Note that steady state was sometimes difficult to reach.

At steady state, one can observe the C.W. lasing and the mode-locking thresholds, single pulse as well as stable multi-pulses and temporally modulated pulsed train. We have computed the spectrum and the pulse temporal profile everywhere in the cavity for our different laser configurations. The results are in good agreement with the experimental data

#185913 - $15.00 USD Received 25 Feb 2013; revised 17 Apr 2013; accepted 20 Apr 2013; published 25 Apr 2013

(see Table 1 and Fig. 3, 4 and 5). Finally, we stress that the model can take into account modifications of almost all the experimental parameters. Therefore, it can be used as a numerical tool to improve and to scale-up the performance of these lasers. More details about this model will be given elsewhere.

5. Conclusion

In conclusion, self mode-locked high power oscillator with widely adjustable pulse duration ranging from 20 ps down to 130 fs has been demonstrated. It takes advantage of the high gain and the management of NPE and spectral filtering taking place in the laser. We have demonstrated that such laser is able to deliver almost dispersion free picoseconds pulses at high repetition rate and with a high averaged intensity. This indicates that controlling the NPE and spectral filtering makes it possible to both adjust the central frequency, the pulse duration and pulse shape over a broad spectral and temporal domain.

Acknowledgment

This work was partly supported by the Conseil Régional Aquitaine (CRA) and the Association Nationale de la Recherche Technique (ANRT).

#185913 - $15.00 USD Received 25 Feb 2013; revised 17 Apr 2013; accepted 20 Apr 2013; published 25 Apr 2013